Ore Geology Reviews 81 (2017) 1–9

Contents lists available at ScienceDirect

Ore Geology Reviews

journal homepage: www.elsevier.com/locate/oregeorev

Ultrafine particles in ground sulfide ores: A comparison of four Cu-Ni ores from Siberia, Russia

Yuri Mikhlin [a,*], Alexander Romanchenko [a], Sergey Vorobyev [a], Sergey Karasev [a], Mikhail Volochaev [c], Evgeny Kamenskiy [a], Ekaterina Burdakova [b]

[a] Institute of Chemistry and Chemical Technology of the Siberian Branch of the Russian Academy of Sciences, Akademgorodok, 50/24, Krasnoyarsk 660036, Russia
[b] Siberian Federal University, Svobodny pr. 79, Krasnoyarsk 660041, Russia
[c] Kirensky Institute of Physics of the Siberian Branch of the Russian Academy of Sciences, Akademgorodok 50/38, Krasnoyarsk 660036, Russia

ARTICLE INFO

Article history:
Received 7 August 2016
Received in revised form 12 October 2016
Accepted 21 October 2016
Available online 24 October 2016

Keywords:
Cu-Ni sulfide ores
Ultrafine particles
Mineral surfaces
Colloids
Beneficiation
Environment

ABSTRACT

Nano-, submicro- and micrometer mineral particles may have an important role in beneficiation of metal ores and environmental impact, but their origin and characteristics are poorly understood. Here, we report data for the yield and the composition of fine fractions, and surfaces of several ground Cu-Ni sulfide ores studied using laser diffraction, scanning electron microscopy and energy dispersive X-ray analysis, X-ray photoelectron spectroscopy. Colloidal particles were characterized using dynamic light scattering, zeta-potential measurement, transmission electron microscopy and electron diffraction. The production of fines by dry milling was found to increase from about 0.01 vol.% to 0.2 vol.% for submicrometer particles and from ~0.5 vol.% to about 1.5 vol.% for particulate material less than 5 μm in the following order: Noril'sk disseminated low sulfide ore ≤ Noril'sk Cu-rich sulfide ore < Noril'sk valleriite ore < Kingash ore. For wet milling, the yield may be several times higher. Both surfaces of the milled ores and colloids were enriched in O, Mg, Si (largely as serpentine slimes) and depleted in sulfur, basic metals and iron, but colloidal valleriite, chalcopyrite, and oxidized pyrrhotite were found in the respective supernatants too. Typically, the colloidal particles form aggregates with an average hydrodynamic diameter of about 1 μm and a smaller number of ~5 μm species, except for valleriite ore, which exhibits a single size distribution peak at 2.7 μm. Zeta-potential, which characterizes the electric charge of the particles and dispersion stability of colloids, changed from −25 mV for the low sulfide ore to about 0 mV for valleriite ore, and to +15 mV for Kingash ore. Poor flotation recovery of metal from Kingash ore and Noril'sk valleriite ore is suggested to be due to both the large quantities and positive charge of hydrophilic ultrafine serpentine and/or magnesium hydroxide minerals. Resistance to oxidation and hence stability against aggregation of copper-bearing sulfide colloids in waste waters is expected to result in a negative impact on the environment.

1. Introduction

The efficiency of processing of sulfide ores of base and precious metals depends not only on grade, chemical and mineralogical composition but also on the texture of the ore, including grain size, hardness, and intergrowth of sulfide and gangue minerals. It is also necessary to take into consideration particle size distributions of ground ores, which is difficult to predict from geological analysis and mineralogical characterization. Recovery of metal from sulfide ores commonly involves crushing and grinding the ore to the particle size ranging from 20 μm to 100 μm in order to liberate minerals before the separation. Flotation recovery of smaller sulfide particles usually decreases, mainly due to a slow bubble–particle attachment, and notable quantities of metals can be lost to the tailings (Albijanic et al., 2010; Feng and Aldrich, 1999; Johnson, 2006; Miettinen et al., 2010; Sivamohan, 1990; Subrahmanyam and Forssberg, 1990; Trahar, 1981). In practice, particle size distributions of milled ores are quite wide, comprising particles of both metal sulfide and gangue minerals ranging in size from micrometer through submicrometer to nanometer scale. These ultrafine particles can accumulate in water produced from the mill, increasing viscosity of slurries, being entrained into flotation froth, etc., or can deposit on mineral surfaces affecting their characteristics. Generally, these phenomena are weakly controllable and have a detrimental effect on the flotation performance (Bremmell et al., 2005; Edwards et al., 1980; George et al., 2004; Grano, 2009; Feng et al., 2012, 2016; Kirjavainen and Heiskanen, 2007; Miettinen et al., 2010; Peng and Grano, 2010; Pietrobon et al., 1997; Senior and Thomas, 2005). The ultrafine particles then go into metal concentrates or enter tailing, waste waters, mine and natural drainage, and contribute to the formation of dust, which pollutes the atmosphere, soils, surface- and ground waters (Crane and Scott, 2012; Fu and Wang, 2011; Hudson-Edwards, 2003; Plathe et al.,

* Corresponding author.
E-mail address: yumikh@icct.ru (Y. Mikhlin).

http://dx.doi.org/10.1016/j.oregeorev.2016.10.024
0169-1368/

2013; Wang et al., 2014). Aquatic (colloidal) nano- and micrometer-size particles transport various elements and substances in the environment in often larger quantities than dissolved species (Boyd, 2010; Gammons and Frandsen, 2001; Hochella et al., 2008; Hofacker et al., 2013; Hotze et al., 2010; Luther and Rickard, 2005; Rozan et al., 2000; Wang, 2014; Weber et al., 2009; Wigginton et al., 2007). The amount of ultrafine solids, including sulfides and oxides of toxic heavy metals derived from mineral industry, is expected to be much higher than, for instance, from emerging engineered nanomaterials, which presently attract considerable attention (Auffan et al., 2010; Cornelis et al., 2014; Garner and Keller, 2014; Mudunkotuwa and Grassian, 2011).

The formation of very fine-grained particulate material in the course of grinding of sulfide ores, and its fate in the environment require investigation in a variety of different ore types. In a recent study on Gorevskoe Pb-Zn sulfide ore (Mikhlin et al., 2016a), it was found that the yields of submicrometer particles and those less than 5 μm approach several tenths of vol.%, and a few vol.%, respectively. In this study, four samples from Cu-Ni and platinum group elements (PGE) bearing sulfide ores located at Krasnoyarsk territory in Siberia (Russia) were studied after drum milling. Three of them are the most important types of Noril'sk Deposits of Siberia (Dodin, 2002; Krivolutskaya, 2016); they comprise a high-grade Cu-Ni sulfide ore, disseminated low sulfide ore, and valleriite-rich "coppery" ore containing copper and sulfur largely as a layered metal sulfide/hydroxide mineral valleriite, $4(Cu,Fe)\cdot 3(Mg,Al)(OH)_2$ (Evans and Allmann, 1968; Gubaidulina et al., 2007; Harris et al., 1970; Hughes et al., 1993; Laptev et al., 2009; Li and Cui, 1994). The disseminated ores of the lower portions of layered intrusions of gabbro-dolerite rock make up about 84% of total reserves at Noril'sk (several billion tons); Cu-rich, or "massive", sulfide ores (about 9% of the deposits) are located in metamorphosed rocks surrounding the intrusions; and the coppery ores (about 7% of the total reserves) form veins in sedimentary and metamorphic rocks on the margins of the massive ores. Valleriite-rich ore, however, has not typically being processed in the past due to technological problems (Laptev et al., 2009). A low sulfide Ni-Cu ore is from Kingash deposit located in Eastern Sayan; sulfides are mainly disseminated in the ultrabasic rocks, including metamorphized varieties (serpentenites) (Glazunov and Radomskaya, 2010; Lygin, 2010). Kingash ore cluster, the overall resources of which amount to 5.5 million tons of nickel and 2.3 million tons of copper (Lygin, 2010), is not in commercial exploitation till now, in part because of poor flotation performance that can be caused by gangue serpentine minerals (Algebraistova et al., 2012; Edwards et al., 1980; Feng et al., 2012, 2016; Kirjavainen and Heiskanen, 2007; Miettinen et al., 2010; Pietrobon et al., 1997; Senior and Thomas, 2005). The aim of the current research was to investigate granulometric distribution, composition, and surface characteristics of various fractions of the ground ores, with emphasis on potential effect of ultrafine particles, including colloids, on the technological processes and the environment.

2. Experimental study

2.1. Sulfide ore samples and preparation

Noril'sk Cu- and Ni-rich sulfide ore (Oktyabrskiy deposit) is composed of hexagonal pyrrhotite Fe_9S_{10}, and chalcopyrite ($CuFeS_2$), cubanite ($CuFe_2S_3$), and pentlandite [$(Ni,Fe)_9S_8$]. The main elements are Fe (25–38 wt.%), S (25–30 wt.%), Cu (4–12 wt.%), Si (about 5 wt.%), with the content of Mg is as low as ~1%. The elemental compositions of representative samples of this and other ores determined using EDX analysis are given in Table 1 (see also Electronic Supplementary Information). The disseminated sulfide ore from Noril'sk-I deposit has much lower concentrations of sulfur (1–3 wt.%), iron (8–12 wt.%), heavy metals (Cu 2–3 wt.%, Ni 0.2–0.5 wt.%), whereas the amounts of Si, Al, and Mg approach 20 wt.%, 6–8 wt.%, and 7–10 wt.%, respectively. The sulfide minerals (pyrrhotite, chalcopyrite, pentlandite) are associated with gabbro dolerite rocks enriched with magnesian olivine and pyroxene (Grinenko, 1985; Krivolutskaya, 2016). Valleriite ore (Talnakh deposit) contains a large amount of sulfur (about 10 wt.%), iron (10–15%), copper and nickel (up to 10 wt.% and 1–2 wt.%, respectively), along with high Mg concentration (about 18 wt.%), and a lesser abundance of Si (up to 10%), and Al (below 3 wt.%). The content of valleriite is about 20%; the main other sulfide minerals are pyrite, chalcopyrite, pentlandite, and pyrrhotite. The ore samples also contain serpentine (largely lizardite $Mg_3Si_2O_5(OH)_4$), silicates, magnetite. Kingash ore from Upper Kingash deposit (average elemental concentrations, wt.%: Mg 22, Si 15, Al 1.1, Fe 7.6, Cu 0.6, Ni 0.3, S 1.0) is composed of up to 70–75% of serpentine minerals and iron and non-ferrous metals as magnetite (10–12%), chalcopyrite, pentlandite, and pyrrhotite (about 4% total). In all of the ores about 80% of non-ferrous metal is associated with sulfide.

Table 1
Surface concentrations (at.%) of main elements in the milled ores and their supernatant particles determined using XPS in comparison with EDX data.

	Fe	Cu	S	Si	Al	Mg	Ca	Cl	Ni	O
Noril'sk Cu-rich ore										
EDX	21.6	6.2	30.6	5.3	2.6	0.87	1.5	–	1.6	28.8
XPS	5.8	1.4	18.9	7.6	4.2	6.0	–	–	0.36	55.7
Supernatant particles	2.7	0.25	4.9	15.2	4.1	6.3	–	–	0.49	65.5
Noril'sk dissemin. ore										
EDX	4.4	0.76	0.88	15.5	5.6	9.7	2.4	–	0.2	59.3
XPS	1.8	tr.	tr.	19.9	6.2	11.6	0.90		–	59.2
Supernatant particles	1.3	0.24	tr.	19.8	4.6	10.3	0.81		–	58.2
Valleriite ore										
EDX	6.8	3.8	8.7	8.3	2.6	18.4	–	–	0.37	51.0
XPS	2.2	0.89	4.7	10.3	4.4	20.3	–	–	–	57.1
Supernatant particles	1.25	0.49	4.0	11.6	4.9	20.3	–	–	–	57.6
Kingash ore										
EDX	2.9	0.21	0.66	11.6	0.84	19.2	0.13	–	0.11	64.3
XPS	0.46	0.07	–	14.8	3.5	22.7	–	0.2	0.06	58.4
Supernatant particles	0.54	0.04	–	15.2	4.08	23.4	0.15	0.25	0.04	56.2

The ore samples were crushed to less than 5 mm and ground in a laboratory drum mill with steel balls using solid/water/balls weight ratio of 1:0.4:9 or dry milled at the solid/balls ratio of 1:10. To prepare the slurries and colloidal particles, the ground ore samples were mixed in distilled water (10 wt.% solid) in a glass beaker for 5 min, and then allowed to sediment at room temperature (22 ± 1 °C) for a predetermined time, typically 40 min. Then a portion of the supernatant liquid was collected by a pipette at approximately 1 cm below the surface of the solution.

2.2. Electron microscopy and related techniques

The ground samples were characterized using scanning electron microscopy (SEM), backscattered electron imaging microanalysis (SEM–BSE), and energy dispersive X-ray analysis (EDX) utilizing a Hitachi TM 3000 instrument operated at acceleration voltage of 15 kV, equipped with a Bruker Quantax 70 EDX analyzer. Transmission electron microscopy images and selected area electron diffraction patterns (SAED) were acquired using a Hitachi S5000 microscope operated at accelerated voltage of 100 kV. Colloidal particles were prepared for TEM investigation by placing the supernatant droplet on a carbon coated copper grid and allowing it to dry at room temperature.

2.3. Laser diffraction, dynamic light scattering and zeta-potential measurement

Laser diffraction analysis with a Horiba LA-300 instrument was employed to determine granulometric composition of mineral particles down to 0.1 μm in aqueous slurries. Particle size and zeta-potential

distributions for colloid particles in supernatants were studied using dynamic light scattering (DLS) (Hassan et al., 2015) and electrophoretic mobility with Zetasizer Nano ZS spectrometer (Malvern Instruments) at 25 °C. Zeta-potential (Delgado et al., 2005) was measured in a folded polycarbonate cell with Pd electrodes, no background electrolyte was added, and no pH adjustment was made.

2.4. X-ray photoelectron spectroscopy (XPS)

X-ray photoelectron spectra were collected using a SPECS spectrometer equipped with a PHOIBOS 150 MCD 9 hemispherical analyzer at electron take-off angle 90^0 at a pressure of 10^{-9} mBar. The Mg Kα irradiation (1253.6 eV) of a dual anode X-ray source was employed for excitation; the pass energies of the analyzer was 20 eV for survey spectra and 8 eV for high-resolution spectra of specific element lines. A low-energy electron flood gun was applied to eliminate inhomogeneous electrostatic charging of the samples; the binding energies were corrected using the C 1s reference (285.0 eV) from aliphatic carbon contamination. The data processing was performed using CasaXPS software package. The surface concentrations of elements were determined from survey spectra; detailed S 2p and other spectra were fitted with Gaussian-Lorentzian peak profiles after Shirley background subtraction (Hofmann, 2013; Wincott and Vaughan, 2006).

3. Results

3.1. Scanning electron microscopy and laser diffraction analysis

Fig. 1 shows typical SEM micrographs of the ground ores; additional SEM images and the element distribution maps can be found in Electronic Supplementary Information file (ESI). Metal sulfide minerals (pyrrhotite and others) having higher conductivity than gangue materials show up as lighter particles. The photomicrographs reveal a large number of finer particles in addition to minerals of 20 μm to 100 μm in size. The surfaces of the larger particles in the rich sulfide ore and the disseminated low sulfide ore samples are virtually free of fines. On the other hand, valleriite ore and Kingash ore comprise considerable amounts of smaller particles, many of which adhered to the coarser particles.

Particle size distributions were measured using laser diffraction analysis, and are shown in Fig. 2 for dry milling for 2 h (curves 1 and 2) and wet milling for 0.5 h (3). The wet milling is more efficient and results in narrower particle distributions and somewhat higher yields of ultrafines, however, it is more sensitive to conditions of milling (time, water content, and so on), making the comparison of different ores more difficult. The main regularities of the production of ultrafines by means of wet and dry grinding were basically similar, and the data on wet grinding are mostly omitted in this article for the sake of brevity.

Despite the size distributions depend on the mode of grinding, differently for various ores, the yield of fine particles is clearly more strongly affected by the type of the ore. Generally, there are two peaks of the particle size distribution at 1–2 μm and 20–50 μm; a similar distribution was found for Pb-Zn sulfide ore (Mikhlin et al., 2016a). The production of the fines for dry grinding increases in the following order: low sulfide disseminated ore ≤ rich sulfide ore < valleriite ore < Kingash ore, varying from less than 0.01 vol.% to 0.2 vol.% for submicrometer particles and from ~0.5 vol.% to about 1.5 vol.% for the fraction less than 5 μm. The effect of wet grinding is illustrated by histograms for Kingash ore (d3, d4) as an example. The very special behavior of valleriite ore appears to be due to exfoliation of brucite-like layers of valleriite and needs more research that will be reported separately. The sample slurries were also ultrasonically treated to avoid aggregation of the particles (dashed curves 2 in the size distribution plots, and columns a2–d2, d4 in the histogram). The sonification moderately increased the quantity of sub-5 μm fines and more notably enhanced that of submicrometer particles, particularly, for the rich sulfide and valleriite ores having the high content of metal sulfides.

3.2. Energy dispersive X-ray analysis and X-ray photoelectron spectroscopy

Table 1 represents the results of EDX analysis (see also Electronic Supplementary Information) that is, in fact, the bulk composition of the samples, in comparison with the surface composition of the ground ores and colloids in the respective supernatants found with XPS. XPS is a surface-sensitive technique with the probing depth of a few nm, allowing to determine the elemental concentrations, and, in principle, the chemical state of atoms and so to identify surface and nanoscale substances (see, for example, Hofmann, 2013, Wincott and Vaughan, 2006). Concentration of carbon originating mainly from surface contaminations was excluded; a fraction of oxygen is related to adsorbed water, carbon-bearing contaminants, etc., so the real content of oxygen in the surface layers of solids seems to be somewhat lower, and the quantities of other elements are slightly underestimated. Fig. 3 shows representative survey spectra and high-resolution spectra of copper, iron and sulfur from the Cu-rich sulfide ore and valleriite ore, both of the ground material and the colloidal matter; the spectra of two other ores can be found in Supplementary Information file.

The surface concentrations generally differ from the bulk compositions owing to oxidation of metal sulfide surfaces, and deposition of fines and slimes. Table 1 shows that the surface layers of all the ores are enriched in Si, Al, Mg and depleted in Fe, Cu, Ni and S. The relative concentrations of the gangue elements, especially Mg, clearly increased for the rich sulfide ore surface but insignificantly changed for the ores with low content of metal sulfides. This indicates that gangue minerals, first of all, magnesium-bearing, precipitate onto sulfide minerals during their milling and suspending in water. The fact that the ultrasonic treatment of the high-sulfur ores significantly increased the quantities of ultrafine particles (Fig. 2) probably indicates that the ultrafines are weakly attached to the surfaces of the sulfides.

The concentrations of sulfur, iron and base metals further decreased in colloidal particles deposited on HOPG from the respective supernatants, indicating that those are largely composed of Si, Mg, Al oxides and minor metal sulfides, approaching the composition of gangue minerals in case of the two low sulfide ores. However, sulfur, iron and copper were found in the colloids in Noril'sk Cu-rich sulfide and valleriite ores. The detailed spectra (Fig. 3) show Cu $2p_{3/2}$ peak at the binding energy (BE) of 932.2 eV for the rich ore, and at 932.7 eV for valleriite ore, and no or very minor shake-up satellite intensities at 944–948 eV, both for the precipitates and colloids. These features are typical for copper (I) in chalcopyrite (Goh et al., 2006; Harmer et al., 2006) and valleriite (the spectra of Noril'sk valleriites will be reported in detail elsewhere), respectively, so these minerals are very likely present in the ultrafine (colloidal) matter. The Fe 2p spectra from rich sulfide ore revealed a larger contribution of Fe(III)-O species at BEs above 710 eV than of Fe-S species at ~708 eV due to substantial oxidation of pyrrhotite surfaces (Pratt et al., 1994; Mycroft et al., 1995; Mikhlin et al., 2000, 2002, 2016b), whereas iron in the supernatant occurs completely as iron oxyhydroxides and/or sulfate; Ni species (see Fig. S1 in Electronic Supplementary Information) are fully oxidized too. The surface iron in valleriite ore is found to be largely in Fe(III)-S form, while the iron-containing sulfides in the colloids are substantially, but not completely, oxidized. The spectra of sulfur can be fitted using three S $2p_{3/2,1/2}$ doublets, with the main S $2p_{3/2}$ peak at 161.2 eV originating from monosulfide anions in pyrrhotite and chalcopyrite, and smaller signals at 162.6 eV, 163 eV from disulfide and polysulfide at metal-deficient surfaces of the oxidized sulfide minerals, and ~169 eV from sulfate (Pratt et al., 1994; Mycroft et al., 1995; Mikhlin et al., 2000, 2002, 2004, 2016b; Harmer et al., 2006). The S 2p spectra of valleriite ore exhibit the major S $2p_{3/2}$ peak at 161.7 eV and minor contributions of oxidized species both for the precipitate and the colloids, showing that valleriite is quite resistant to oxidation. Furthermore, it seems likely that the higher

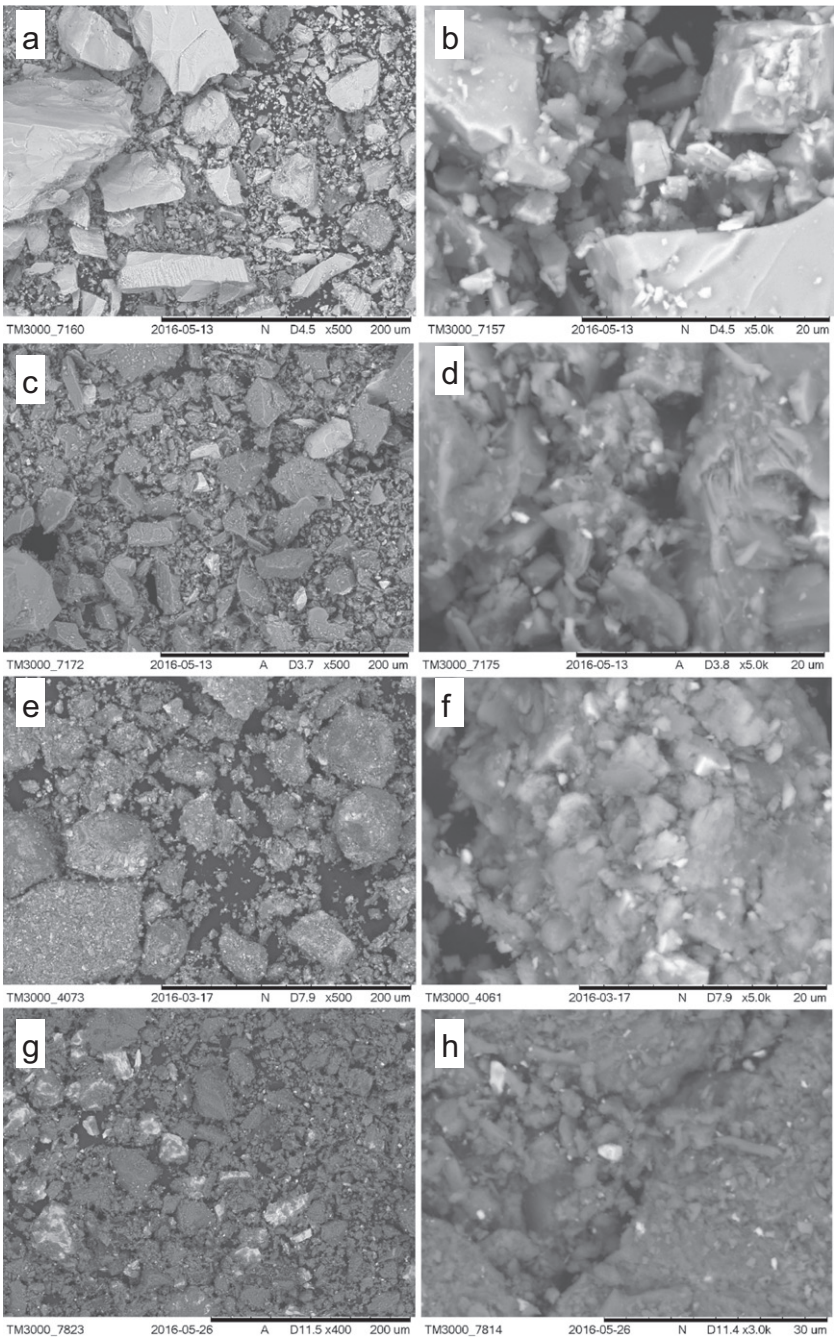

Fig. 1. Typical SEM micrographs with different magnification of ground ores (scale bar is 200 μm for left panels a, c, e, g, 20 μm for images b, d, f and 30 μm for image h): (a, b) Noril'sk Cu-rich sulfide, (c, d) disseminated sulfide ore, (e, f) valleriite ore, (g, h) Kingash ore.

amount of colloidal valleriite is related to the reduced oxidation of mineral surface.

3.3. Characterization of colloidal particles

3.3.1. Dynamic light scattering and zeta-potential measurement

Further insights into the nature and properties of ultrafine materials were gained through DLS and zeta potential analysis of colloids remaining in the supernatants after sedimentation of coarser particles. Fig. 4 shows typical hydrodynamic diameter distributions of the colloids at natural pHs after the precipitation for 40 min. The main maximum of the distribution is located at about 1 μm, it decreased in height and slowly shifted to lesser hydrodynamic diameter with time (not shown in Figures). A second small peak at about 5.5 μm varied in a more complicated way and was probably due to transient aggregates, which are formed from smaller particles prior the precipitation. The mean diameter of the colloidal species in Kingash ore was somewhat larger (~1.3 μm) and the distribution function was broader than those for Noril'sk Cu-rich sulfide ore and disseminated ore. In contrast, valleriite ore exhibited one relatively narrow peak centered at 2.7 μm.

These phenomena can be rationalized by measuring zeta-potential of each supernatant (Fig. 4, right-hand panel), that is the potential difference in the electric double layer between the aqueous medium and the stationary layer of fluid attached to dispersed particles, which characterizes the charge of the surface and the aggregative stability of the particles (Delgado et al., 2005). All the samples show one maximum of zeta-potential distribution, the position of which varied from −25 mV (low sulfide ore) to +15 mV (Kingash ore), and so one sort

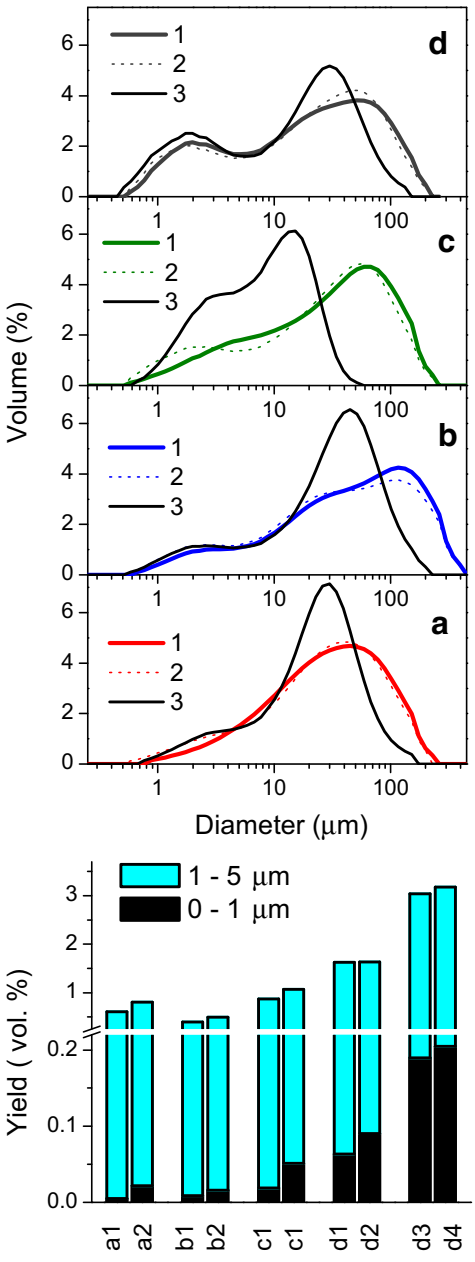

Fig. 2. Particle size distributions of ores (1, 2) dry-milled for 2 h and (3) wet-milled for 0.5 h: (a) Noril'sk Cu-rich sulfide ore, (b) Noril'sk disseminated ore, (c) Noril'sk valleriite ore, (d) Kingash ore determined from laser diffraction analysis. The dotted curves and columns (a2–d2, d4) in the histogram are obtained after ultrasonic treatment for 5 min before the analysis.

of colloidal species predominating in a particular supernatant. The values of zeta-potential stay almost constant with time for all of the ores, despite the gradual coagulation and decreasing the hydrodynamic diameter of the colloids. The small negative zeta-potential of Cu-rich sulfide ore (about −5 mV) can be explained by the abundance of pyrrhotite, which is easily oxidized producing surface Fe(III) oxyhydroxides (Pratt et al., 1994; Mikhlin et al., 2002, 2016b), and so has less negative surface charge than oxidation–resistant metal sulfides (Grano, 2009; Peng and Grano, 2010). In addition, the oxidation generates sulfuric acid (pH of the slurry is 4.5–5), with zeta-potential generally becoming less negative (or more positive) in acidic solutions than in neutral or alkaline media (Delgado et al., 2005). Zeta-potential of colloids in valleriite ore slurries was close to zero (0–+5 mV); interestingly, the same value was found in special experiments with pure valleriite mineral. This low potential (and surface charge) results in weaker repulsion of the particles and a larger size of colloidal aggregates as compared with other ores.

3.3.2. Transmission electron microscopy, electron diffraction, EDX

Fig. 5 shows representative TEM images and selected area electron diffraction (SAED) patterns from dried supernatants of the four ores. The micrographs reveal, in agreement with the above DLS data, numerous aggregates of 1–2 μm in size, which consist of smaller particles. The micrometer- and submicrometer particles of Noril'sk Cu-rich sulfide ore (Fig. 5a, b) and, in a lesser degree, of valleriite ore (Fig. 5g, h) are relatively dense and coated with loose nanoscale products. The results of EDX, XPS, and SAED analysis suggest that the particles of the rich sulfide ore are largely composed of pyrrhotite, along with minor chalcopyrite, pentlandite, etc., the surface of which is oxidized and covered with flake-like Fe(III) oxyhydroxides and sulfates; the sample contained also magnesium-enriched pyroxene silicates.

The SAED patterns (c, f, i, l) consist of several sets of spots from single micro- and nanocrystals, and diffuse rings from randomly orientated small crystallites or/and poor crystalline/amorphous matter. The number of spots (i.e., bigger crystals) is higher in the case of Cu-rich sulfide ore, with the interplanar distances d of 0.30 nm, 0.209 nm, 0.172 nm, 0.132 nm of pyrrhotite (Fig. 5c), and valleriite ore with signals of chalcopyrite and valleriite crystals (Fig. 5i), and it is the lowest for Kingash ore (Fig. 5l). The diffuse rings originating preferentially from lizardite $Mg_3Si_2O_5(OH)_4$ (d = 0.25 nm, 0.43 nm, 0.35 nm, 0.21 nm, 0.15 nm, etc.), are the most intense for colloids of Kingash ore and valleriite ore, and are weaker, although still observable, for Noril'sk disseminated and Cu-rich sulfide ores, reflecting the quantities of very fine serpentine in these colloids.

Additional details can be seen in TEM images obtained at higher magnification (Fig. 6). In particular, thin nano- and submicrometer plates attributable to serpentine group minerals were well observed for Noril'sk valleriite ore and Kingash ore (Fig. 6a). This agrees with the SAED data, and the XPS analysis of the colloids showing the atomic Mg/Si ratio close to 1.5 for Kingash ore and 2 for valleriite ore that contains Mg in brucite-like layers of valleriite. The other interesting colloids found in both these ores are numerous rounded particles varied in diameter from 10 nm to 50 nm (Fig. 6b, c, see also Electronic Supplementary Information, Fig. S6). The intense diffuse reflection at 0.25 nm in the SAED pattern obtained from these regions can be assigned to lizardite, while EDX analysis found, in addition to Mg and Si, comparable quantities of Cl and S. The nanoparticles appear to be a secondary composite product, which may arise due to weathering and oxidation of metal sulfides, including upon the milling, with minor chlorapatite presented in the ore (Glazunov and Radomskaya, 2010) acting as a source of Cl. The quantity of this species is not high (XPS found about 0.2 at.% of Cl in Kingash ore), but the nanoparticles may accumulate in the process water.

4. Discussion

The above results demonstrate that the comminution of the ores, which contain insignificant quantities of ultrafine-grained minerals, produces up to several percents of sub-5 μm particles and 0.2 vol.% of submicrometer particles in the case of dry grinding, and essentially higher amount for wet grinding. The grinding of Kingash ore comprising gangue serpentine and Noril'sk valleriite ore produces several times higher percentage of the ultrafine fractions, probably, owing to enhanced cleavage of serpentines and valleriite. The weight proportion of the fines seems to be somewhat lower than the volume percentage, because the low-size varieties are largely aggregates of submicro- and nanometer particles but not dense solids. The quantities of ultrafine particles are, in fact, larger than those of flotation reagents employed in mineral processing (typically, between 10 g per ton and 1 kg per ton, i.e. 0.001 wt.% and 0.1 wt.%), which also may form nano- and submicrometer-scale particles (Mikhlin et al., 2016c).

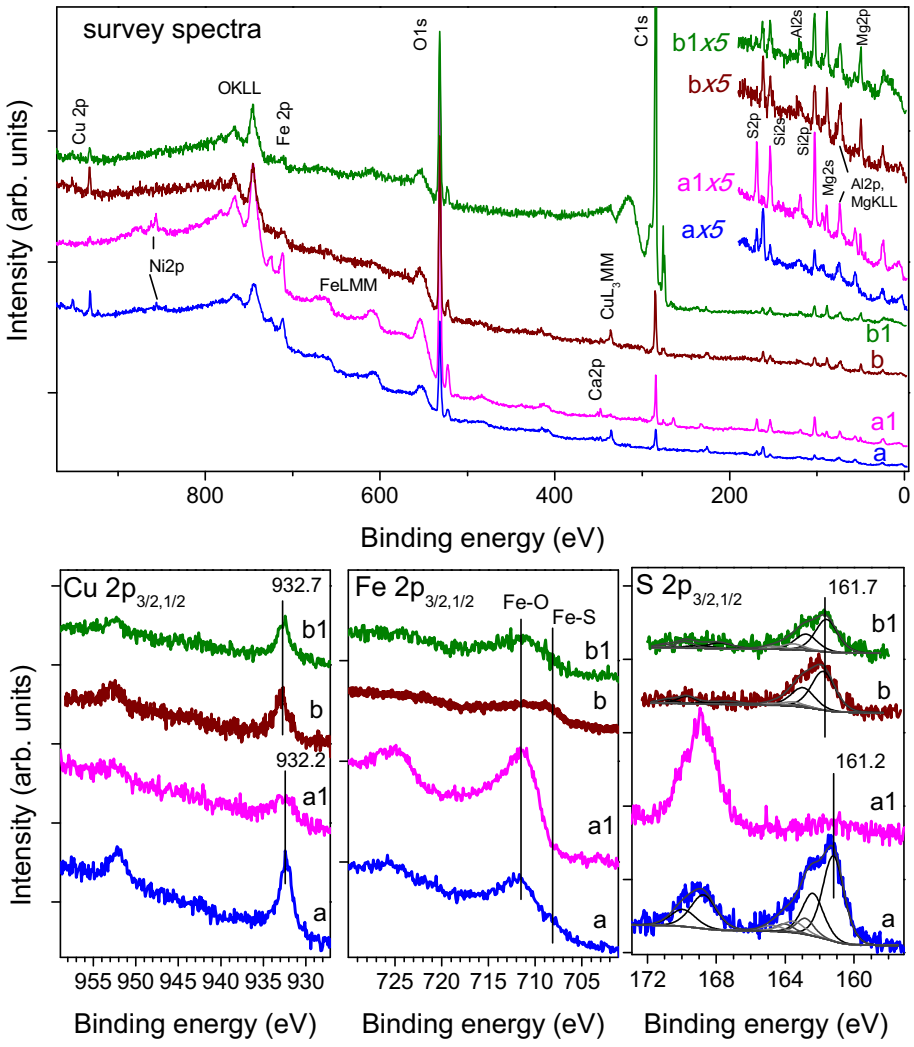

Fig. 3. X-ray photoelectron spectra of (a) Noril'sk Cu-rich sulfide ore and (b) valleriite ore, and the colloidal particles (a1, b1) from their supernatants dried at a highly-oriented pyrographite (HOPG) support. The spectra are shifted vertically for clarity.

The composition of ultrafines derived from ores having low concentration of sulfide (Noril'sk disseminated and Kingash ores) is close to that of gangue, i.e., those are depleted in metal sulfides and somewhat enriched in Mg and Si. The fine fractions of ores with high concentration of sulfur (Noril'sk Cu-rich and valleriite ores) contain substantial quantities of sulfide minerals, particularly pyrrhotite, chalcopyrite and valleriite, with the colloidal sulfides being more oxidized than the coarse particles. It is important that less oxidized metal sulfides show

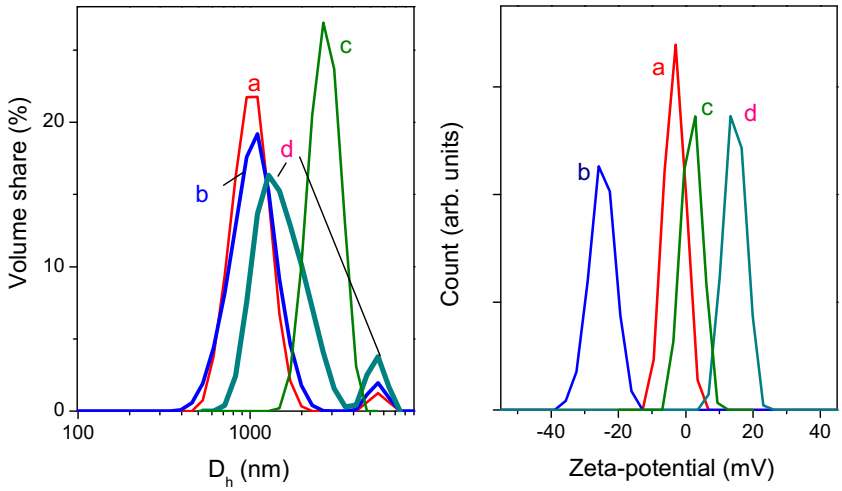

Fig. 4. Typical hydrodynamic diameter (left panel) and zeta-potential distributions of colloidal particles in supernatants above milled ores (solid/liquid ratio of 0.1 g/ml) after 40 min sedimentation: (a) Noril'sk Cu-rich sulfide ore (pH 4.6), (b) Noril'sk disseminated ore (pH 8.5), (c) Noril'sk valleriite ore (pH 7.8), and (d) Kingash ore (pH 9).

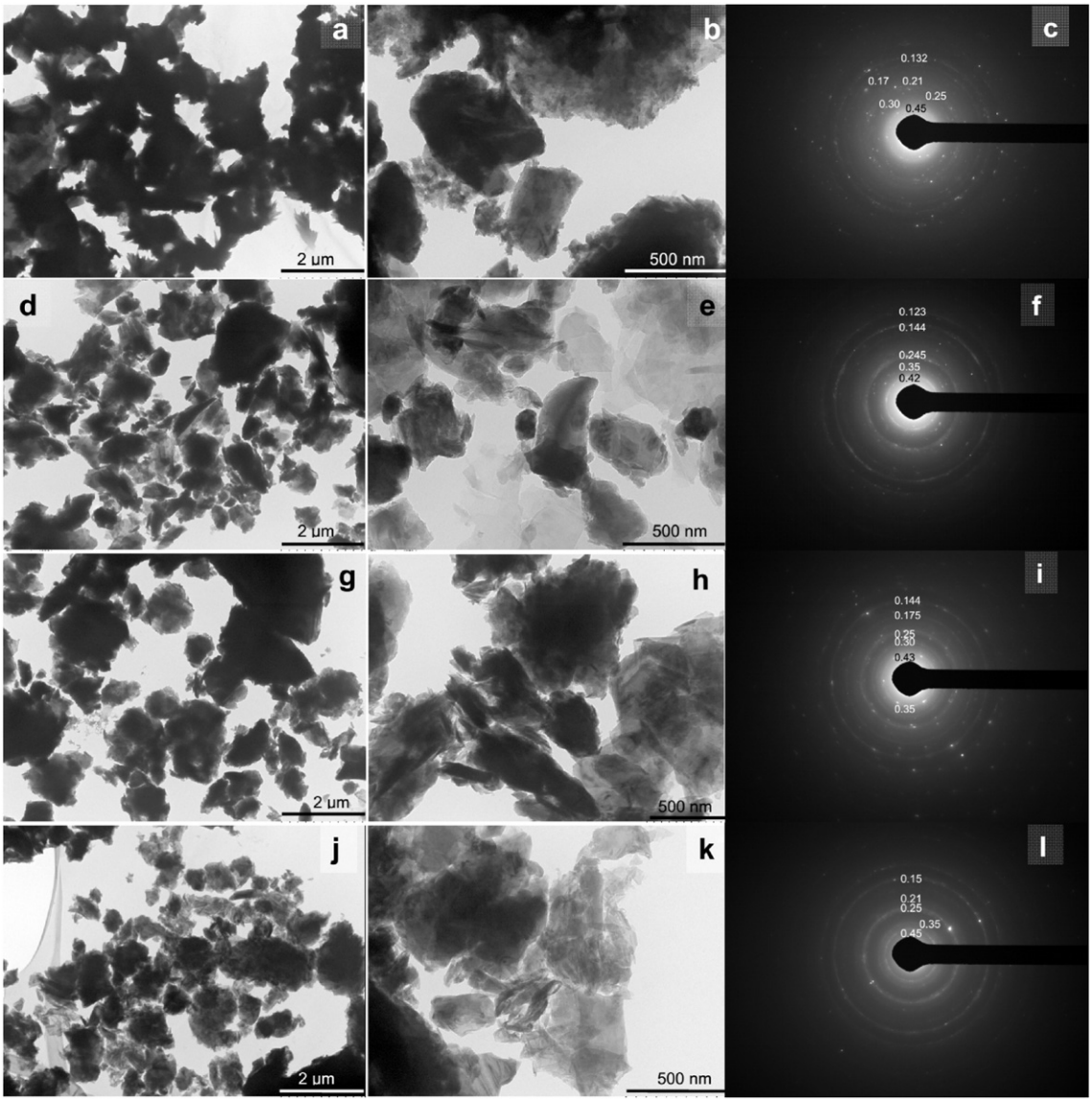

Fig. 5. TEM micrographs with different magnification and electron diffraction patterns (figures stand for main interplanar distances, nm, see text for detail) of colloidal particles in (a–c) Noril'sk Cu-rich sulfide ore, (d–f) disseminated ore, (g–h) valleriite ore, (j–l) Kingash ore.

higher stability against aggregation, which decreases in the order: valleriite > chalcopyrite > (pentlandite) > pyrrhotite. It seems probable that the Cu-bearing sulfide nanoparticles easily release copper cations, which activate the flotation of pyrite, pyrrhotite and other minerals or/and affect the dissolution of minerals, or nanoparticles may act directly by immobilizing on mineral surfaces. Although the yield of the metal sulfide colloids is not high, those could accumulate in the circulating water. On the other hand, mobilization and transportation of heavy metals in surface waters by aquatic metal sulfide nanoparticles, and their impact on biota are revealed in many studies (for example,

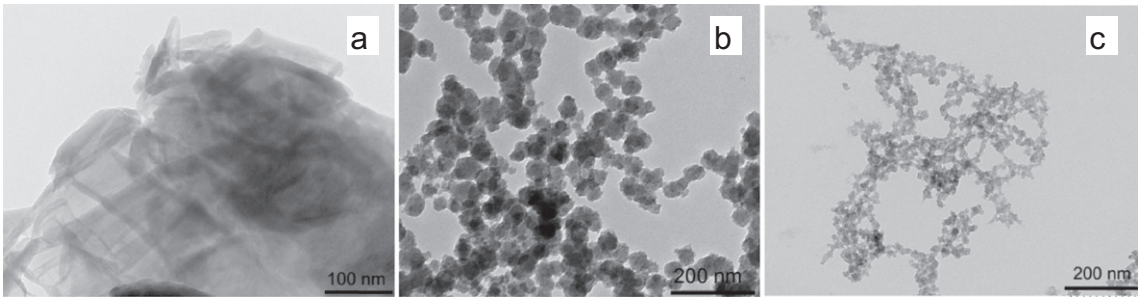

Fig. 6. TEM micrographs of colloids found in supernatants of (a, b) Kingash ore and (c) valleriite ore, attributable to nanoplates of serpentine (a) and composite nanoparticles (b, c).

Hudson-Edwards, 2003; Banfalvi, 2006; Wigginton et al., 2007; Weber et al., 2009; Boyd, 2010; Hotze et al., 2010; Fu and Wang, 2011; Hashim et al., 2011; Hofacker et al., 2013; Plathe et al., 2013; Wang, 2014), so decontamination of waste waters of the mineral industry from colloids is essential.

Positive zeta-potential of colloidal particles in Kingash ore is due to magnesium silicates (lizardite and others), which tend to form hydrophilic coatings at negatively charged sulfide surfaces through electrostatic attraction in the neutral and slightly alkaline aqueous media, decreasing the rate of flotation and the recovery of valuable minerals (Bremmell et al., 2005 and references therein). To reduce the negative influence, a number of reagents, which adsorb either at the sulfides or at the gangue particles, or facilitate sedimentation of serpentine have been proposed but the problem is not completely solved yet (Edwards et al., 1980; Pietrobon et al., 1997; Bremmell et al., 2005; Kirjavainen and Heiskanen, 2007; Feng et al., 2016). The slight positive charge of colloids in valleriite ore slurries seems to result from brucite-like layers of valleriite rather than minor serpentine. The low recovery of valleriite and its detrimental effect on sulfide flotation can be due to magnesium hydroxide colloids, which form due to the exfoliation, but this requires further research. We suggest that the recovery of sulfides is low due not only to the positive charge of gangue minerals but that also critically depends on abundance of the submicrometer particles, and sharply decreases as their quantity exceeds 0.01–0.02 vol.% (100–200 g/ton) and so the content of flotation reagents. Technological aspects of the problem, however, go beyond the framework of this article.

5. Conclusions

We studied ultrafine fractions of four Cu-Ni sulfide ores produced by conventional drum milling with steel balls. It was found that for dry milling the yield varies from ~0.01 vol.% to 0.2 vol.% for submicrometer particles and from ~0.5 vol.% to about 1.5 vol.% for sub-5 μm ones, and increases in the following order: Cu-rich sulfide ore ≤ low sulfide ore < valleriite ore < Kingash ore. The production of fines in wet milling may be several times higher, especially for valleriite ore. The ultrafine fractions were enriched in Mg, Si, O, particularly because of increased content of serpentine minerals (mainly lizardite), and depleted in S, Fe, basic metals, although colloidal valleriite and chalcopyrite were present in supernatants too. Hydrodynamic diameter distributions of the colloidal aggregates for three ores showed main maxima at about 1 μm and minor one at about 5.5 μm, whereas valleriite ore exhibited one maximum at 2.7 μm. Zeta potential of colloids at natural pH 8–9 was −25 mV for Noril'sk low sulfide ore, −5 mV for rich sulfide ore (pH 4.5), 0–+5 mV for valleriite ore, and +15 mV for Kingash ore. The low flotation recovery of heavy metals from Kingash ore and Noril'sk valleriite ore is believed to be due to both the positive charge and large quantities of hydrophilic ultrafine magnesian mineral particles depositing onto metal sulfides. Resistance to oxidation and hence aggregative stability of colloids increases in the order valleriite > chalcopyrite > (pentlandite) > pyrrhotite. This may result in accumulation of particles bearing copper and other metals in the mill water and their impact on the environment.

Acknowledgements

This research was supported by the Russian Science Foundation, grant no. 14-17-00280.

Appendix A. Supplementary data

Supplementary data to this article can be found online at doi:10.1016/j.oregeorev.2016.10.024.

References

Albijanic, B., Ozdemir, O., Nguyen, A.V., Bradshaw, D., 2010. A review of induction and attachment times of wetting thin films between air bubbles and particles and its relevance in the separation of particles by flotation. Adv. Colloid Interf. Sci. 159, 1–21.
Algebraistova, N.K., Perfileva, N.S., Markova, S.A., Razvayznaya, A.V., Groo, E.A., Kondratieva, A.A., Macshanin, A.V., 2012. The development combinative ore-dressing scheme of Kingash ore. J. Siberian Fed. Univ. Eng. Technol. 7:777–782. http://krsk.elib.sfu-kras.ru/bitstream/2311/9534/1/10_Algebraistova.pdf (In Russian).
Auffan, M., Bottero, J.Y., Chaneac, C., Rose, J., 2010. Inorganic manufactured nanoparticles: how their physicochemical properties influence their biological effects in aqueous environments. Nanomedicine 5, 999–1007.
Banfalvi, G., 2006. Removal of insoluble heavy metal sulfides from water. Chemosphere 63, 1231–1234.
Boyd, R.S., 2010. Heavy metal pollutants and chemical ecology: exploring new frontiers. J. Chem. Ecol. 36, 46–58.
Bremmell, K.E., Fornasiero, D., Ralston, J., 2005. Pentlandite–lizardite interactions and implications for their separation by flotation. Colloids Surf. A Physicochem. Eng. Asp. 252, 207–212.
Cornelis, G., Hund-Rinke, K., Kuhlbusch, T., van den Brink, N., Nickel, C., 2014. Fate and bioavailability of engineered nanoparticles in soils: a review. Crit. Rev. Environ. Sci. Technol. 44, 2720–2764.
Crane, R.A., Scott, T.B., 2012. Future prospects for an emerging water treatment technology. J. Hazard. Mater. 211−212, 112–125.
Delgado, A.V., González-Caballero, F., Hunter, R.J., Koopal, L.K., Lyklema, J., 2005. Measurement and interpretation of electrokinetic phenomena (IUPAC technical report). Pure Appl. Chem. 77, 1753–1805.
Dodin, D.A., 2002. Metallogeniya Taimyro-Noril'skogo regiona (Metallogeny of Taimyr-Noril'sk region). Nauka, St.-Petersburg (in Russian).
Edwards, C.R., Kipkie, W.B., Agar, G.E., 1980. The effect of slime coatings of the serpentine minerals, chrysotile and lizardite, on pentlandite flotation. Int. J. Miner. Process. 7, 33–42.
Evans Jr., H.T., Allmann, R., 1968. The crystal structure and crystal chemistry of valleriite. Z. Krist. 127, 73–93.
Feng, D., Aldrich, C., 1999. Effect of particle size on flotation performance of complex sulphide ores. Miner. Eng. 12, 721–731.
Feng, B., Feng, Q., Lu, Y., Lv, P., 2012. The effect of conditioning methods and chain length of xanthate on the flotation of a nickel ore. Miner. Eng. 39, 48–50.
Feng, B., Lu, Y., Feng, Q., 2016. Interactions and depression of chlorite and serpentine. Chinese J. Rare Metals 40, 167–171.
Fu, F., Wang, Q., 2011. Removal of heavy metal ions from wastewaters: a review. J. Environ. Manag. 92, 407–418.
Gammons, C.H., Frandsen, A.K., 2001. Fate and transport of metals in H_2S-rich waters at a treatment wetland. Geochem. Trans. 2, 1–15.
Garner, K.L., Keller, A.A., 2014. Emerging patterns for engineered nanomaterials in the environment: a review of fate and toxicity studies. J. Nanopart. Res. 16, 2503.
George, P., Nguyen, A.V., Jameson, G.J., 2004. Assessment of true flotation and entrainment in the flotation of submicron particles by fine bubbles. Miner. Eng. 17, 847–853.
Glazunov, O.M., Radomskaya, T.A., 2010. Geochemical model of genesis of the Kingash platinoid–copper–nickel deposit. Dokl. Earth Sci. 430 (1), 71–75.
Goh, S., Buckley, A., Lamb, R., Rosenberg, R., Moran, D., 2006. The oxidation states of copper and iron in mineral sulfides, and the oxides formed on initial exposure of chalcopyrite and bornite to air. Geochim. Cosmochim. Acta 70, 2210–2228.
Grano, S., 2009. The critical importance of the grinding environment on fine particle recovery in flotation. Miner. Eng. 22, 386–394.
Grinenko, L.I., 1985. Sources of sulfur of the nickeliferrous and barren gabbro-dolerite intrusions of the northwest Siberian platform. Int. Geol. Rev. 27, 695–708.
Gubaidulina, T.V., Chistyakova, N.I., Rusakov, V.S., 2007. Mössbauer study of layered iron hydroxysulfides: tochilinite and valleriite. Bull. Russ. Acad. Sci. Phys. 71, 1269–1272.
Harmer, S.L., Thomas, J.E., Fornasiero, D., Gerson, A.R., 2006. The evolution of surface layers formed during chalcopyrite leaching. Geochim. Cosmochim. Acta 70, 4392–4402.
Harris, D.C., Cabry, L.J., Stewart, J.M., 1970. A "valleriite-type" mineral from Noril'sk, Western Siberia. Am. Mineral. 55, 2110–2114.
Hashim, M.A., Mukhopadhyay, S., Sahu, J.N., Sengupta, B., 2011. Remediation technologies for heavy metal contaminated groundwater. J. Environ. Manag. 92, 2355–2388.
Hassan, P.A., Rana, S., Verma, G., 2015. Making sense of brownian motion: colloid characterization by dynamic light scattering. Langmuir 31, 3–12.
Hochella Jr., M.F., Lower, S.K., Maurice, P.A., Penn, R.L., Sahai, N., Sparks, D.L., Twining, B.S., 2008. Nanominerals, mineral nanoparticles, and earth systems. Science 319, 1631–1635.
Hofacker, A.F., Voegelin, A., Kaegi, R., Weber, F.A., Kretzschmar, R., 2013. Temperature-dependent formation of metallic copper and metal sulfide nanoparticles during flooding of a contaminated soil. Geochim. Cosmochim. Acta 103, 316–332.
Hofmann, S., 2013. Auger- and X-ray Photoelectron Spectroscopy in Materials Science. A User-oriented Guide. Springer-Verlag, Berlin Heidelberg.
Hotze, E.M., Phenrat, T., Lowry, G.V., 2010. Nanoparticle aggregation: challenges to understanding transport and reactivity in the environment. J. Environ. Qual. 39, 1909–1924.
Hudson-Edwards, K.A., 2003. Sources, mineralogy, chemistry and fate of heavy metal-bearing particles in mining-affected rivers systems. Mineral. Mag. 67, 205–217.
Hughes, A.E., Kakos, G.A., Turney, T.W., Williams, T.B., 1993. Synthesis and structure of valleriite, a layered metal hydroxide/sulfide composite. J. Solid State Chem. 104, 422–436.
Johnson, N.W., 2006. Liberated 0–10 μm particles from sulphide ores, their production and separation—recent developments and future needs. Miner. Eng. 19, 666–674.
Kirjavainen, V., Heiskanen, K., 2007. Some factors that affect beneficiation of sulphide nickel–copper ores. Miner. Eng. 20, 629–633.

Krivolutskaya, N.A., 2016. Siberian Traps and Pt-Cu-Ni Deposits in the Noril'sk Area. Springer, Cham Heidelberg New York Dordrecht London (364 p.).
Laptev, Y.V., Shevchenko, V.S., Urakaev, F.K., 2009. Sulphidation of valleriite in SO_2 solutions. Hydrometallurgy 98, 201–205.
Li, R., Cui, L., 1994. Investigations on valleriite from Western China: crystal chemistry and separation properties. Int. J. Miner. Process. 41, 271–283.
Luther III, G.W., Rickard, D.T., 2005. Metal sulfide cluster complexes and their biogeochemical importance in the environment. J. Nanopart. Res. 7, 389–407.
Lygin, A.V., 2010. Peculiar features of ore composition of the upper Kingash PGE-Co–Cu–Ni deposit (Krasnoyarsk territory). Mosc. Univ. Geol. Bull. 65 (2), 130–133.
Miettinen, T., Ralston, J., Fornasiero, D., 2010. The limits of fine particle flotation. Miner. Eng. 23, 420–437.
Mikhlin, Y., Varnek, V., Asanov, I., Tomashevich, Y., Okotrub, A., Livshits, A., Selyutin, G., Pashkov, G., 2000. Reactivity of pyrrhotite (Fe_9S_{10}) surfaces: spectroscopic studies. Phys. Chem. Chem. Phys. 2, 4393–4398.
Mikhlin, Y.L., Kuklinskiy, A.V., Pavlenko, N.I., Varnek, V.A., Asanov, I.P., Okotrub, A.V., Selyutin, G.E., Solovyev, L.A., 2002. Spectroscopic and XRD studies of the air degradation of acid-reacted pyrrhotites. Geochim. Cosmochim. Acta 66, 4077–4087.
Mikhlin, Y.L., Tomashevich, Y.V., Asanov, I.P., Okotrub, A.V., Varnek, V.A., Vyalikh, D.V., 2004. Spectroscopic and electrochemical characterization of the surface layers of chalcopyrite ($CuFeS_2$) reacted in acidic solutions. Appl. Surf. Sci. 225, 395–409.
Mikhlin, Y., Vorobyev, S., Romanchenko, A., Karasev, S., Karacharov, A., Zharkov, S., 2016a. Ultrafine particles derived from mineral processing: a case study of the Pb-Zn sulfide ore with emphasis on lead-bearing colloids. Chemosphere 147, 60–66.
Mikhlin, Y., Vorobyev, S., Saikova, S., Tomashevich, Y., Fetisova, O., Kozlova, S., Zharkov, S., 2016b. Preparation and characterization of colloidal copper xanthate nanoparticles. New J. Chem. 40, 3059–3065.
Mikhlin, Y., Tomashevich, Y., Vorobyev, S., Saikova, S., Romanchenko, A., Félix, R., 2016c. Hard X-ray photoelectron and X-ray absorption spectroscopy characterization of oxidized surfaces of iron sulfides. Appl. Surf. Sci. 387, 796–804.
Mudunkotuwa, I.A., Grassian, V.H., 2011. The devil is in the details (or the surface): impact of surface structure and surface energetics on understanding the behavior of nanomaterials in the environment. J. Environ. Monit. 13, 1135–1144.
Mycroft, J.R., Nesbitt, H.W., Pratt, A.R., 1995. X-ray photoelectron and Auger electron spectroscopy of air-oxidized pyrrhotite: distribution of oxidized species with depth. Geochim. Cosmochim. Acta 59, 721–733.
Peng, Y., Grano, S., 2010. Dissolution of fine and intermediate sized galena particles and their interactions with iron hydroxide colloids. J. Colloid Interface Sci. 347, 127–131.
Pietrobon, M.C., Grano, S.R., Sobieraj, S., Ralston, J., 1997. Recovery mechanisms for pentlandite and MgO-bearing gangue minerals in nickel ores from Western Australia. Miner. Eng. 10, 775–786.
Plathe, K.L., von der Kammer, F., Hassellöv, M., Moore, J.N., Murayama, M., Hofmann, T., Hochella Jr., M.F., 2013. The role of nanominerals and mineral nanoparticles in the transport of toxic trace metals: field-flow fractionation and analytical TEM analyses after nanoparticle isolation and density separation. Geochim. Cosmochim. Acta 102, 213–225.
Pratt, A.R., Muir, I.J., Nesbitt, H.W., 1994. X-ray photoelectron and Auger electron studies of pyrrhotite and mechanism of air oxidation. Geochim. Cosmochim. Acta 58, 827–841.
Rozan, T.F., Lassman, M.E., Ridge, D.P., Luther III, G.W., 2000. Evidence for iron, copper and zinc complexation as multinuclear sulphide clusters in oxic rivers. Nature 406, 879–882.
Senior, G.D., Thomas, S.A., 2005. Development and implementation of a new flowsheet for the flotation of a low grade nickel ore. Int. J. Miner. Process. 78, 49–61.
Sivamohan, R., 1990. The problem of recovering very fine particles in mineral processing—a review. Int. J. Miner. Process. 28, 247–288.
Subrahmanyam, T.V., Forssberg, K.S.E., 1990. Fine particles processing: shear-flocculation and carrier flotation — a review. Int. J. Miner. Process. 28, 247–288.
Trahar, W.J., 1981. A rational interpretation of the role of particle size in flotation. Int. J. Miner. Process. 8, 289–327.
Wang, Y., 2014. Nanogeochemistry: nanostructures, emergent properties and their control on geochemical reactions and mass transfers. Chem. Geol. 378–379, 1–23.
Wang, C., Harbottle, D., Liu, Q., Xu, Z., 2014. Current state of fine mineral tailings treatment: a critical review on theory and practice. Miner. Eng. 58, 113–131.
Weber, F.-A., Voegelin, A., Kaegi, R., Kretzschmar, R., 2009. Contaminant mobilization by metallic copper and metal sulphide colloids in flooded soil. Nat. Geosci. 2, 267–271.
Wigginton, N.S., Haus, K.L., Hochella Jr., M.F., 2007. Aquatic environmental nanoparticles. J. Environ. Monit. 9, 1306–1316.
Wincott, P.L., Vaughan, D.J., 2006. Spectroscopic studies of sulfides. Rev. Mineral. Geochem. 61, 181–229.